第 31 卷第 9 期
2015 年 9 月

无 机 化 学 学 报
CHINESE JOURNAL OF INORGANIC CHEMISTRY

Vol.31 No.9
1761-1773

周边硅笼取代的混杂酞菁卟啉三层铽单分子磁体

张 璐[1] 曾涞源[2] 刘 涛[3] 孙君善[1] 窦建民*,[2] 姜建壮*,[1]

([1]北京科技大学化学与生物工程学院,功能分子与晶态材料科学与应用北京市重点实验室,北京 100083)

([2]聊城大学化学系,聊城 252004)

([3]大连理工大学,精细化工国家重点实验室,大连 116012)

摘要:通过在铽的酞菁卟啉混杂三层的卟啉周边共价连接体积庞大的笼型倍半硅氧烷 (POSS),得到了首个包含 POSS 的混杂三层 $Tb_2(Pc)[T(OPOSS)_4PP]_2$ (**1**) [H_2Pc =phthalocyanine; $H_2T(OPOSS)_4PP$ =5,10,15,20-tetra {[[*N*-[heptakis(isobutyl)propoxy]phenyl] octasiloxane]}porphyrin]。为了对比研究,同时合成了类似的三层化合物 $Tb_2(Pc)(TPP)_2$(**2**)(H_2TPP=5,10,15,20-tetraphenyporphyrin)。尤其值得注意的是,在没有外加磁场的条件下,$Tb_2(Pc)[T(OPOSS)_4PP]_2$(**1**)和 $Tb_2(Pc)(TPP)_2$(**2**)分别表现出单分子磁体和非单分子磁体的性质,这充分说明了共价连接均匀分布的 POSS 基团有效地分离了磁性核心,从而改善了酞菁卟啉混杂三层的磁性。

关键词:四吡咯化合物;三明治;POSS;分子杂化;单分子磁体

中图分类号:O614.341; O645.16+2 **文献标识码**:A **文章编号**:1001-4861(2015)09-1761-13

DOI:10.11862/CJIC.2015.190

Mixed Tetrapyrrole Terbium Triple-Decker Single Molecule Magnets with Bulky Inorganic Polyhedral Oligomeric Silsesquioxanes Moieties at Outer Porphyrin Peripheries

ZHANG Lu[1] ZENG Su-Yuan[2] LIU Tao[3] SUN Jun-Shan[1] DOU Jian-Min*,[2] JIANG Jian-Zhuang*,[1]

([1]*Beijing Key Laboratory for Science and Application of Functional Molecular and Crystalline Materials, Department of Chemistry, University of Science and Technology Beijing, Beijing* 100083, *China*)

([2]*Department of Chemistry, Liaocheng University, Liaocheng,* 252004, *China*)

([3]*State Key Laboratory of Fine Chemicals, Dalian University of Technology, Dalian,* 116012, *China*)

Abstract: Bulky inorganic polyhedral oligomeric silsesquioxanes (POSS) moieties were introduced onto the porphyrin periphery in mixed (phthalocyaninato) (porphyrinato) terbium molecule, giving POSS-involved hybrid triple-decker complex $Tb_2(Pc)[T(OPOSS)_4PP]_2$ (**1**) [H_2Pc =phthalocyanine; $H_2T(OPOSS)_4PP$ =5,10,15,20-tetra {[[*N*-[heptakis (isobutyl)propoxy]phenyl]octasiloxane]}porphyrin]. For com- parative study, triple-decker analogue $Tb_2(Pc)(TPP)_2$ (**2**) (H_2TPP=5,10,15,20-tetraphenyporphyrin) was also prepared and structurally characterized. In particular, $Tb_2(Pc)[T(OPOSS)_4PP]_2$ (**1**) and $Tb_2(Pc)(TPP)_2$ (**2**) were revealed to display intrinsic single molecule magnet (SMM) and non-SMM (or field-induced) characteristic, respectively, at zero Oe (or a 3.0 Oe ac field), clearly indicating the effect of the covalently linked, homogenously dispersed POSS moieties on effectively separating the magnetic cores and improving the magnetic property of triple-decker compounds. CCDC: 989974, **2**.

Key words: tetrapyrrole; sandwich POSS; molecular hybrid; single molecule magnet

收稿日期:2015-04-01。收修改稿日期:2015-05-22。

国家自然科学基金(No.21290174),国家重点基础研究发展计划(973 计划)(No.2013CB933402 和 No.2012CB224801)。

*通讯联系人。E-mail:jianzhuang@ustb.edu.cn,jmdou@lcu.edu.cn

0 Introduction

Single molecule magnets (SMMs) were first noticed in early 1990s when a molecular metal coordination compound $Mn_{12}Ac$ was found to retain magnetization for a long time without an external field at liquid-helium temperature [1]. In recent years, SMMs have attracted increasing interest because of their potential to develop new technological applications including storage and process of digital information with high density and unprecedented speed, the molecular-scale spintronic devices and quantum computing at the molecular level[2].

Investigations reveal that the energy barrier in reversing magnetization for SMMs is mainly related with the magnetic anisotropy projected on the ground exchange and the multiplet projection of the total spin on the symmetry axis [1c,3]. In addition, the intermolecular magnetic dipole-dipole interaction, which may result in quantum tunneling of the magnetization (QTM), can also influence the magnetic properties of SMMs as exemplified by lowering of the block temperature [4]. To solve this problem, a physical dilution method by means of the isostructural diamagnetic analogues to dope the paramagnetic SMMs is usually employed[5]. However, a large amount of diamagnetic analogues is necessary for the purpose of effectively dispersing the diamagnetic counterparts around the paramagnetic molecules to weaken the intermolecular magnetic dipole-dipole interaction [4a,6]. An alternative method of such a physical dilution way appears to introduce bulky diamagnetic moieties around the magnetic core by covalently linking. This, however, has not been employed to diminish the magnetic dipole-dipole interaction and in turn to suppress the QTM effect in this field, to the best of our knowledge.

In the present paper, we describe the design and synthesis of the first POSS-involved hybrid triple-decker complex $Tb_2(Pc)[T(OPOSS)_4PP]_2$ (**1**) [H_2Pc = phthalocyanine; $H_2T(OPOSS)_4PP$=5,10,15,20-tetra{[[*N*-[heptakis(isobutyl)propoxy]-phenyl]octasiloxane]}porphyrin]. For the purpose of comparative studies, corresponding triple-decker analogue $Tb_2(Pc)(TPP)_2$ (H_2TPP=5,10,15,20-tetraphenyporphyrin) (**2**) was also prepared and structurally characterized. In particular, comparative studies clearly reveal the effect of the covalently linked, homogenously dispersed bulky POSS moieties on effectively separating the magnetic cores and improving the magnetic property of triple-decker compounds as indicated by the intrinsic SMM and non-SMM nature of $Tb_2(Pc)[T(OPOSS)_4PP]_2$ (**1**) and $Tb_2(Pc)(TPP)_2$ (**2**), respectively, at zero Oe.

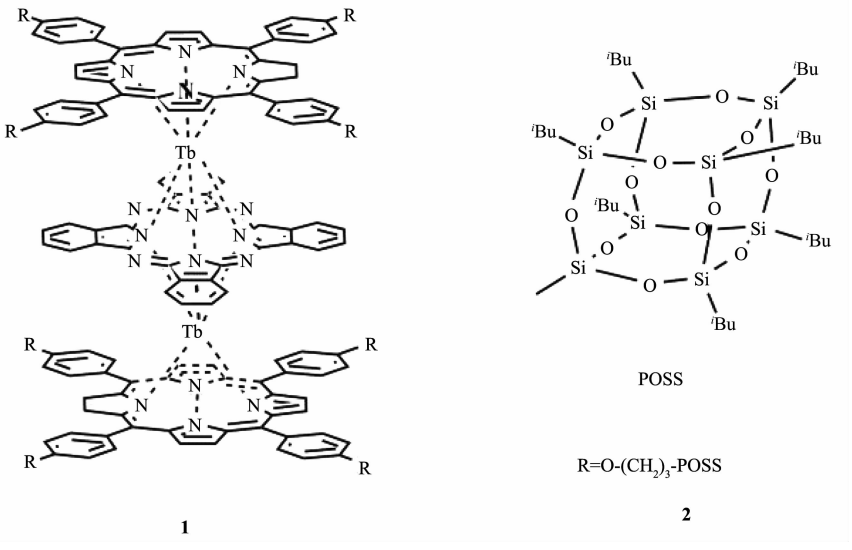

Scheme 1 Schematic molecular structure of POSS-involved hybrid trilple-decker complex $Tb_2(Pc)[T(OPOSS)_4PP]$ (**1**)

1 Experimental

1.1 General Remarks

The trisilanollsobutyl POSS was purchased from Hybrid Plastics (Hattiesburg, MS, USA). Tetrahydrofuran (THF) was freshly distilled using Na with diphenyl ketone coloration under nitrogen atmosphere. *N*,*N*-dimethylformamide (DMF) was freshly distilled with CaH_2 under nitrogen atmosphere. 1,2,4-Trichlorobenzene (TCB) was freshly distilled with CaH_2 under nitrogen atmosphere. Column chromatography was carried out on silica gel (Merck, Kieselgel 60, 63 μm~210 μm (70~230 mesh)) with the indicated eluents. All other reagents and solvents were used as received. The compounds of $Y(acac)_3 \cdot nH_2O$ (acac=acetylacetone), $Tb(acac)_3 \cdot nH_2O$, Li_2Pc (H_2Pc=phthalocyanine), chloropropylisobutyl POSS, 5,10,15,20-tetrakis(4-hydroxyphenyl)porphyrin and 5,10,15,20-tetraphenyporphyrin, and $Y_2(Pc)(TPP)_2$ (H_2TPP=5,10,15,20-tetra-phenyporphyrin) were prepared according to the literature procedure[7-9].

The ^1H NMR spectra were recorded on a Bruker DPX 400 spectrometer in $CDCl_3$ with shifts referenced to $SiMe_4$ (0.00 ppm). Electronic absorption spectra were recorded on a Hitachi U-4100 spectrophotometer. IR spectra were recorded in KBr pellets with 2 cm^{-1} resolution using a Bruker Tensor 37 spectrometer. MALDI-TOF mass spectra were taken on a Bruker BIFLEX III ultra-high resolution Fourier transform ion cyclotron resonance (FT-ICR) mass spectrometer with alpha-cyano-4-hydroxy cinnamic acid as the matrix. Elemental analyses were performed on an Elementar Vavio El Ⅲ. Crystal data for compound **2** were determined by X-ray diffraction analysis at 150 K using Oxford Diffraction Gemini E system with Cu $K\alpha$ radiation λ=0.154 18 nm, and details of the structure refinement are given in Table 1. Magnetic measurements were performed on a Quantum Design MPMS XL-5 SQUID magnetometer on multicrystalline samples. Data were corrected for the diamagnetism of the samples using Pascal constants and of the sample holder by measurement.

CCDC: 989974, **2**.

1.2 Synthesis of 5, 10, 15, 20-tetra{[[N-[heptakis (isobutyl)propoxy] phenyl] octa siloxane]} porphyrin H_2[T(OPOSS)$_4$PP]

The mixture of 5,10,15,20-tetrakis(4-hydroxyphenyl)porphyrin (34 mg, 0.050 mmol) and K_2CO_3 (60 mg, 0.40 mmol) in dry DMF (200 mL) was refluxed under ~3 $cm^3 \cdot min^{-1}$ of N_2 stream at 80 ℃ for 1 h. To which were added chloropropylisobutyl POSS (284 mg, 0.32 mmol) dissolved in dry THF (20 mL) and NaI (68 mg, 0.32 mmol). The resulting mixture was stirred at 80 ℃ for 24 h. After being cooled to room temperature, the reaction mixture was extracted with chloroform and then chromatographed on a silica gel column using $CHCl_3$ as the eluent to give a violet band, which was further purified using gel chromatography with $CHCl_3$ as eluent followed by recrystallization from $CHCl_3$ and MeOH, providing a dark violet solid with the yield of 19.1 mg (9%). ^1H NMR (400 MHz, $CDCl_3$): δ 0.612~0.689(d, 56H, ^{i}Bu-CH_2), 0.965~0.981 (t, 8H, γ propoxy-CH_2), 1.000~1.017 (d, 168H, ^{i}Bu-CH_3), 1.868~1.973 (m, 28H, ^{i}Bu-CH), 2.067~2.124 (m, 8H, β propoxy-CH_2), 4.216~4.249 (t, 8H, α propoxy -CH_2), 7.260~8.114 (d, 16H, Ph-H), 8.855 (d, 8H,

Table 1　Crystal data and structure refinements of compound 2

Compound	**2**	Z	2
Formula	$C_{124}H_{76}Cl_{12}N_{16}Tb_2$	θ range / (°)	3.43~63.81
Formula weight	2 533.25	D_c / ($g \cdot cm^{-3}$)	1.595
Crystal system	Tetragonal	μ / mm^{-1}	9.790
Space group	*I*4/*m*	F(000)	2 532
a / nm	1.431 55(10)	R_1 ($I>2\sigma(I)$)	0.067 0
b / nm	1.431 55(10)	wR_2 ($I>2\sigma(I)$)	0.183 5
c / nm	2.574 25(5)	wR_2 for all	0.191 4
V / cm^3	5.275 50(11)	GOF on F^2	1.049

pyrrole-H). MALDI-TOF MS: an isotopic cluster peaking at *m/z* 4 110.77; Calcd. for $C_{168}H_{202}N_4O_{52}Si_{32}$, 4 108.38. Anal. Calcd. (%) for $C_{168}H_{202}N_4O_{52}Si_{32}$: C, 49.11; H, 7.41; N, 1.36; Found: C, 49.20; H, 7.04; N, 1.08

1.3 Synthesis of $Tb_2(Pc)[T(OPOSS)_4PP]_2$ (1)

A mixture of $H_2[T(OPOSS)_4PP]$ (41 mg, 0.01 mmol) and $[Tb(acac)_3]\cdot nH_2O$ (8 mg, 0.02 mmol) in TCB (1.5 mL) was refluxed at 210 ℃ under ~3 $cm^3\cdot min^{-1}$ of N_2 stream for 4 h. The resulting dark cherry-red solution was cooled to room temperature, then Li_2Pc (2.6 mg, 0.005 mmol) was added. The mixture was refluxed at 210C for a further 6 h, then the solvent was removed under reduced pressure. The reddish brown residue was applied on a silica gel column with $CHCl_3$/hexane (2∶1, *V*/*V*) as the eluent to give a dark violet band, which was further purified using gel chromatography with $CHCl_3$ as eluent followed by recrystallization from $CHCl_3$ and MeOH, giving a dark green solid with the yield of 17.6 mg (29%). ^{1}H NMR (400 MHz, $CDCl_3$): −92.658 (s, 8H, Pc-α H), −90.178 (s, 8H, endo-*ortho* phenyl-H), −47.517 (s, 8H, Pc-β H), −42.527 (s, 16H, pyrrole-H), −31.500 (s, 8H, endo-*meta* phenyl−H), −5.886 and −5.657 (s, 48H, propoxy-H), −2.911 (s, 56H, ^{i}Bu-CH_2), −2.339 (s, 168H, ^{i}Bu-CH_3), −1.605 (s, 28H, ^{i}Bu-CH), −1.424 (s, 56H, ^{i}Bu-CH_2), −0.741~−0.734 (d, 168H, ^{i}Bu-CH_3), −0.258~−0.241 (d, 28H, ^{i}Bu-CH), 12.771 (s, 8H, exo-*meta* phenyl-H), 52.937 (s, 8H, exo-*ortho* phenyl-H). MALDI-TOF MS: an isotopic cluster peaking at *m/z* 9 059.98; Calcd. for $C_{368}H_{616}N_{16}O_{104}Si_{64}Tb_2$, 9 044.20. Anal. Calcd. (%) for $C_{368}H_{616}N_{16}O_{104}Si_{64}Tb_2$: C, 48.87; H, 6.87; N, 2.48; Found: C, 48.71; H, 6.72; N, 2.09.

1.4 Synthesis of $Tb_2(Pc)(TPP)_2$ (2)

By means of the above-mentioned procedure employed to prepare triple-decker **1** with a mixture of $H_2(TPP)$ (6.1 mg, 0.01 mmol) instead of $H_2[T(OPOSS)_4PP]$ as starting material, the target triple-decker compound $Tb_2(Pc)(TPP)_2$ (**2**) (5.0 mg, 39%) was obtained. Single crystals of **2** suitable for X-ray diffraction analysis were grown from slow diffusion of methanol into the $CHCl_3$ solution of this compound. ^{1}H NMR (400 MHz, $CDCl_3$): −94.308 (s, 8H, Pc-α H), −92.655 (s, 8H, endo-*ortho* phenyl-H), −48.691 (s, 8H, Pc-β H), −42.987 (s, 16H, pyrrole-H), −32.120 (s, 8H, endo-*meta* phenyl-H), −6.537 (s, 8H, para phenyl-H) 13.638 (s, 8H, exo-*meta* phenyl-H), 54.820(s, 8H, exo-*ortho* phenyl-H). MALDI-TOF MS: an isotopic cluster peaking at *m/z* 2 056.90; Calcd. for $C_{120}H_{72}N_{16}Tb_2$, 2 055.81. Anal. Calcd. (%) for $C_{120}H_{72}N_{16}Tb_2\cdot CHCl_3\cdot 2CH_3OH$: C, 65.97; H, 3.65; N, 10.00; Found: C, 65.78; H, 3.45; N, 9.65.

2 Results and discussion

2.1 Synthesis and Characterization

As a new class of condensed three-dimensional oligomeric organosiliceous compounds with cage framework, polyhedral oligomeric silsesquioxanes (POSS) have attracted increasing interests in recent years for the synthesis of organic-inorganic molecular hybrid materials[10]. However, despite the recent preparation of quite a number of novel POSS-containing molecular hybrid materials including MCM-POSS[11a], C_{60}-POSS[11b], and graphene-POSS[11c], the POSS-containing molecular hybrid materials with porphyrin as organic component still remain extremely rare, limited to Zn[T(POSS)$_4$PP] (5,10,15,20-tetrakis{[[*N*-[heptakis (isobutyl)propyl] benzamidato]octasiloxane]phenyl} porphyrinato zinc) and Zn[M(POSS)PP] (5-{[[*N*-heptakis (isobutyl)propyl]benzamidato]phenyl} octasiloxane-10, 15, 20-tris(4-tert-butylphenyl)porphyrinato zinc)[12], to the best of our knowledge. In the present case, the metal free 5,10,15,20- tetrakis(4-hydroxyphenyl)porphyrin H_2[T(OH)PP] was prepared according to published procedures[7]. Treatment of H_2[T(OH)PP] with K_2CO_3 followed by reaction with chloropropylisobutyl POSS[8] affords the porphyrin-POSS molecular hybrid, namely metal free 5, 10, 15, 20-tetra{[[*N*-[heptakis(isobutyl)propoxy]phenyl] octasiloxane]}porphyrin $H_2[T(OPOSS)_4PP]$. Reaction between $H_2[T(OPOSS)_4PP]$ and $[Tb(acac)_3]\cdot nH_2O$ *in situ* generates the monomeric intermediate Tb[T(OPOSS)$_4$ PP](acac), which reacts with Li_2Pc in 1,2,4-trichlorobenzene (TCB) to give mixed (phthalocyaninato) (porphyrinato) triple-deckers $Tb_2(Pc)[T(OPOSS)_4PP]_2$ (**1**) in the yield of 39% (Scheme 1). For comparative study, mixed (phthalocyaninato) (porphyrinato) triple-decker

analogue Tb_2 (Pc) $(TPP)_2$ (**2**) (H_2TPP =5,10,15,20-tetraphenyporphyrin) was also prepared following the same procedure. Satisfactory elemental analysis results were obtained for these newly prepared triple-decker compounds after repeatedly column chromatographic purification followed by recrystallization (Table 2). The MALDI-TOF mass spectra of these compounds clearly show intense signals for the molecular ion $[M]^+$. The isotopic patterns closely resemble those of the simulated ones given in Fig.1.

2.2 Structure of 2

Compound **2** crystallizes in the tetragonal system with an *I*4/*m* space group with two triple-deckers per unit cell. The crystal data are summarized in Table 1.

Fig.2 shows the molecular structure of **2** in two different perspective views. In this triple-decker compound, each terbium center is octa-coordinated by the pyrrole and isoindole nitrogen atoms of an outer TPP and the inner Pc rings, respectively, confirming the ligand arrangement of [(TPP)Tb(Pc)Tb(TPP)] in the triple-decker molecule. The two terbium centers are identical in terms of their coordination geometry and separation from the ligands. The twist angle, defined as the rotation angle of one macrocycle away from the eclipsed conformation of the two macrocycles, between Pc ring and TPP ring is 3.59°. The Pc ring locates exactly in the middle of the two terbium atoms with the distance between the outer TPP and the inner Pc rings of 0.310 2 nm. Both terbium centers lie closer to the TPP ring due to its larger central cavity in comparison with the Pc ligand, 0.123 9 vs. 0.186 3 nm, Table 3, with the intramolecular Tb…Tb distance amounting to 0.373 6 nm, indicating the presence of significant intramolecular dipole-dipole interaction

Table 2　Mass spectroscopic and elemental analysis data for the compounds H_2[T(OPOSS)$_4$PP], Tb_2(Pc)[T(OPOSS)$_4$PP]$_2$, Tb_2(Pc)[TPP]$_2$[a]

Compound	Molecular Formula	Yield / %	M^+ (m/z)[b]	Analysis / %[a,b]		
				C	H	N
H_2[T(OPOSS)$_4$PP]	$C_{168}H_{302}N_4O_{52}Si_{32}$	9	4 110.77 (4 108.38)	49.20 (49.11)	7.04 (7.41)	1.08 (1.36)
1	$C_{368}H_{616}N_{16}O_{104}Si_{64}Tb_2$	39	9 059.98 (9 044.20)	48.71 (48.87)	6.72 (6.87)	2.09 (2.48)
2	$C_{120}H_{72}N_{16}Tb_2$	39	2 056.90 (2 055.81)	65.78 (65.97)	3.45 (3.65)	9.65 (10.00)

[a] Calculated values given in parentheses. [b]By MALDI-TOF mass spectrometry. The value corresponds to the most abundant isotopic peak of the protonated molecular ion

Table 3　Comparison of the structural data for 2

	2[c]
Tb-N(TPP) bond distance / nm	0.240 2
Tb-N(Pc) bond distance / nm	0.260 8
Tb-N_4(TPP) plane distance / nm	0.123 9
Tb-N_4 Pc plane distance / nm	0.186 3
Interplanar distance / nm	0.310 2
Tb_1-Tb_2 distance / nm	0.372 6
Dihedral angle between the N_4(TPP) and N_4(Pc) planes / (°)	0
Dihedral angle ϕ for the TPP ring / (°)[a]	12.03
Dihedral angle ϕ for the Pc ring / (°)[a]	0
Average twist angle / (°) [b]	3.59

[a]The average dihedral angle of the individual pyrrole or isoindole ring with respect to the corresponding N_4(TPP) or N_4(Pc) mean planes.

[b]Defined as the rotation angle of one macrocycle away from the eclipsed conformation of the two macrocycles.

[c]The data are mean value of those for compound **2**

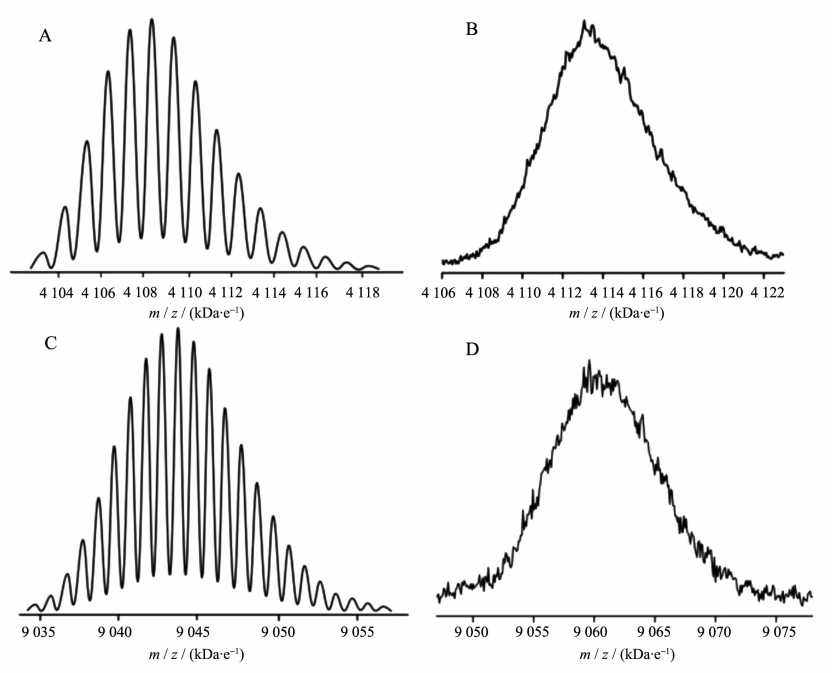

Fig.1 (A) Experimental and (B) simulated isotopic pattern shown in the MALDI-TOF mass spectrum of H_2[T(OPOSS)$_4$PP], (C) Experimental and (D) simulated isotopic pattern shown in the MALDI-TOF mass spectrum of Tb_2(Pc)[T(OPOSS)$_4$PP]$_2$

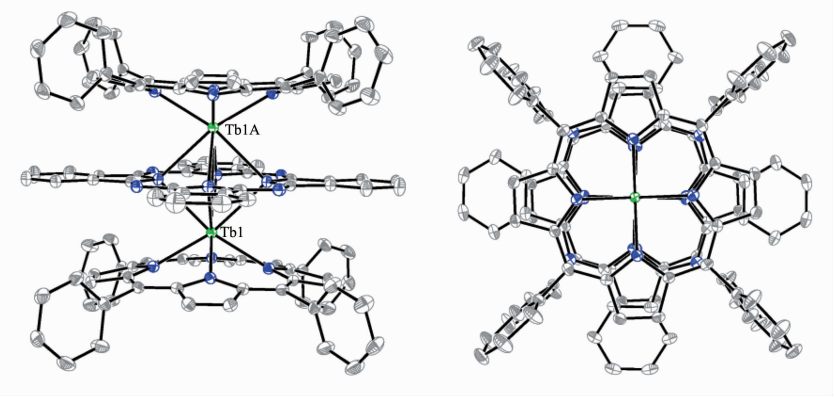

Fig.2 Molecular structure of **2** in side view and top view with hydrogen atoms omitted and the ellipsoids drawn at the 30% probability levels (Tb(Ⅲ) green, C gray, N blue)

between the two Tb atoms.

In the crystal of $Tb_2(Pc)(TPP)_2$ (**2**), the adjacent triple-decker molecules are connected by the solvent $CHCl_3$ molecule to form a two dimensional (2D) structure depending on the C-H ⋯ Cl hydrogen bonding interaction between the C-H bond of the porphyrin phenyl group and the chlorine atom of $CHCl_3$ with the nearest intermolecular Tb ⋯ Tb distance of 1.431 6 nm, Fig.3. These 2D structures are further packed into three dimensional (3D) structure depending on Van der Waals interaction (Fig.4), with the nearest inter-molecular Tb ⋯ Tb distance of 1.364 2 nm. These long intermolecular terbium ionic distances seem to suggest the lack of the intermolecular dipole-dipole interaction between Tb ions. However, as detailed below, the non-SMM nature revealed for this compound at zero Oe, in combination with the typical SMM characteristic of the same compound after dilution with the diamagnetic $Y_2(Pc)(TPP)_2$, clearly indicates the presence of intermolecular dipole-dipole interaction between Tb ions and its effect on its magnetic properties. This appears in line with the previous investigation results that the dipole-dipole interaction between Tb ions with the

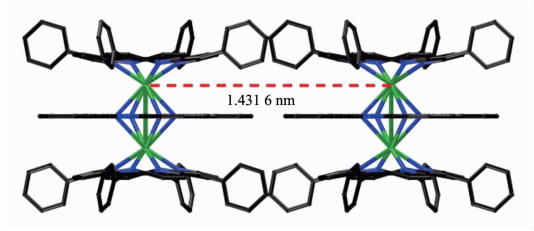

Fig.3　Two dimensional packing plots of **2** in side view

distance of 1.16 nm still cannot be neglected[4b,13].

Repeated trials fail to afford single crystals of the POSS-involved hybrid triple-decker complex $Tb_2(Pc)[T(OPOSS)_4PP]_2$ (**1**) suitable for X-ray diffraction analysis despite the great efforts paid thus far.

As can be seen in Figs. 5 and 6, involvement of two paramagnetic terbium ions in these compounds induces observation of significantly broadened signals. For the triple-decker compound **2** without the POSS moieties, the signal observed at δ =−94.308 and −48.691 can be assigned to the non-peripheral and peripheral protons of the Pc ring respectively, the signal at δ =−42.987 is attributed to the pyrrole protons of the TPP ligand, while the signals at δ = −92.655, −32.120, −6.537, −13.638, and 54.820 are due to the protons in the phenyl moieties of the porphyrin ligand, Fig.5. This seems also true for the triple-decker analogue **1** with POSS moieties attached at the porphyrin ligand through the *meso*-phenyl groups, Fig.6, with the signals of the Pc protons at δ =−92.658 and −47.678, the signal of the pyrrole protons of the porphyrin ligand observed at δ = −43.368, and the signals of the protons in the aryl moieties of $T(OPOSS)_4PP$ resonating at δ=−90.178, −31.591, 12.775 and 53.302. Additional signals observed at δ =−2.911, −1.424, −2.339, −1.605, −0.741~−0.734, and −0.258~−0.241 in the ^{1}H NMR spectrum of **1** are assigned to the protons in the isobutyl substituents of POSS and the signals appearing at δ=−5.891 and −5.660 to the protons in the propoxy linkers which connect the POSS and porphyrin moieties.

The electronic absorption spectra of the two complexes **1** and **2** recorded in $CHCl_3$ are shown in Fig. 7 and 8. Both triple-decker compounds **1** and **2** exhibit typical feature of the electronic absorption spectra for mixed (phthalocyaninato) (porphyrinato) rare earth triple-decker complexes in the form of (TAP)M(Pc)M

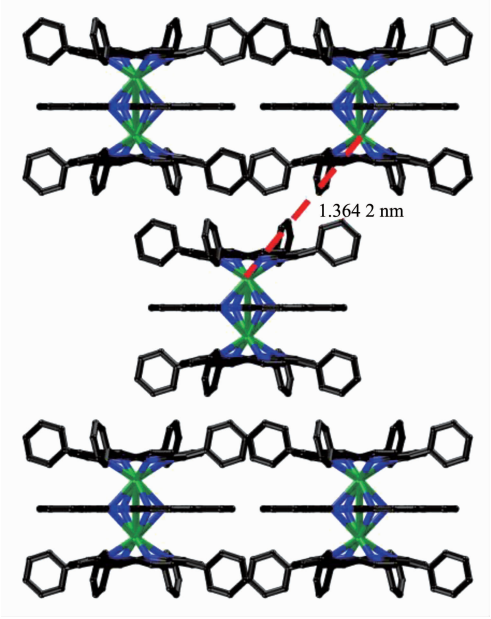

Fig.4　Three dimensional packing plots of **2** in side view

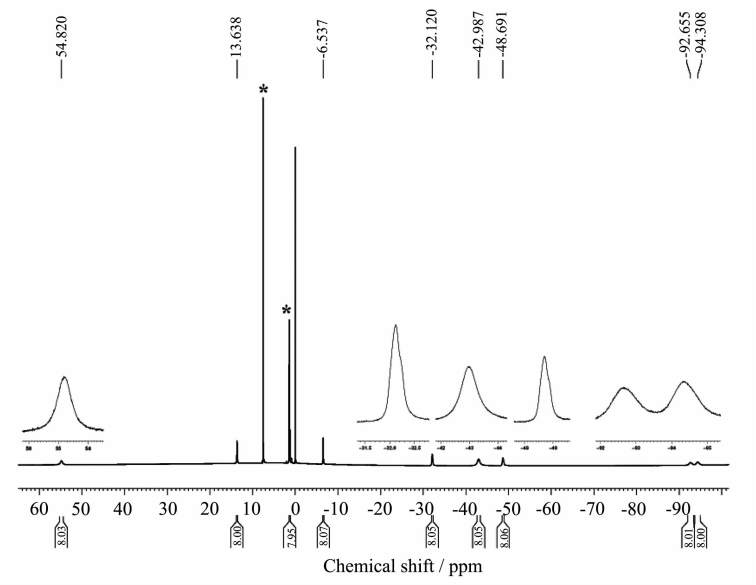

* denotes the solvent impurity

Fig.5 ^{1}H NMR spectra of compound **2** recorded in $CDCl_3$

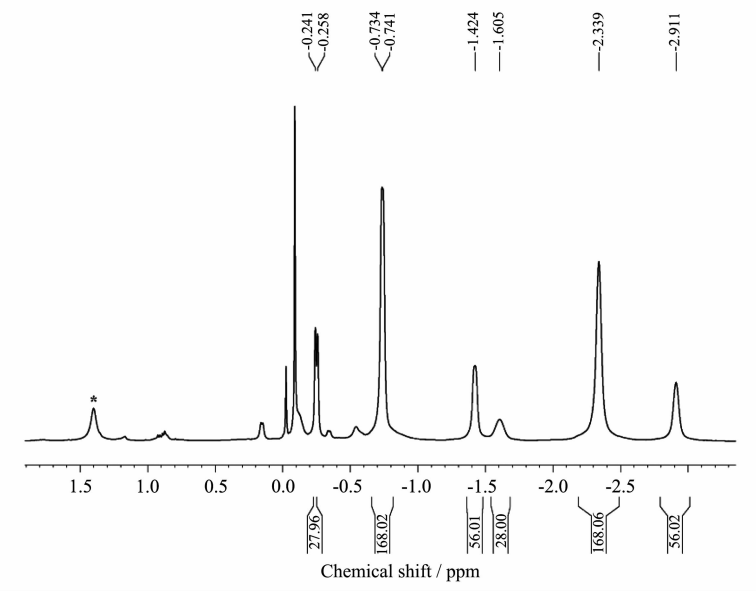

* denotes the solvent impurity

Fig.6 Part of ^{1}H NMR spectra of compound **1** recorded in $CDCl_3$

(TAP) (H_2TAP=5,10,15,20-tetraarylporphyrin) with the tetrapyrrole Soret bands appearing at 352 ~353 and 418~420 nm and Q bands at 492~493, 605~606, and 976~977 nm, respectively[14].

In the IR spectra of triple-decker compounds $Tb_2(Pc)[T(OPOSS)_4PP]_2$ (**1**) and $Tb_2(Pc)(TPP)_2$ (**2**) (Fig.9), the moderately strong band observed at 1 330~1 333 cm^{-1} is attributed to the characteristic IR band for Pc^{2-}[15]. In addition to the absorption bands contributed from the central aromatic Pc and Por macrocycle (including the wagging and torsion vibrations of C-H groups, and the C =N aza group stretching vibrations that are commonly appearing in the spectra of both compounds), the strong absorptions observed at 1 102~1 109 cm^{-1} for $Tb_2(Pc)[T(OPOSS)_4PP]_2$ (**1**) are contributed by the Si-O-Si stretching vibrations and the absorptions at 1 231~1 238 cm^{-1} by the symmetric C-O-C stretching vibrations. It is worth noting that both these absorptions could be observed in the IR spectrum of $Tb_2(Pc)(TPP)_2$ (**2**). This is also true for the most intense

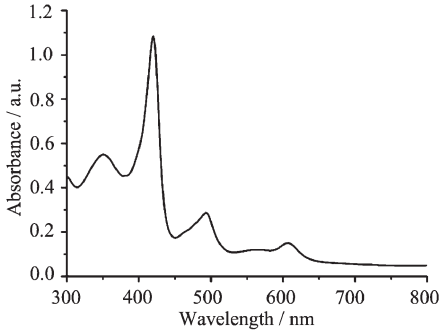

Fig.7　Electronic absorption spectrum of **1** in $CHCl_3$

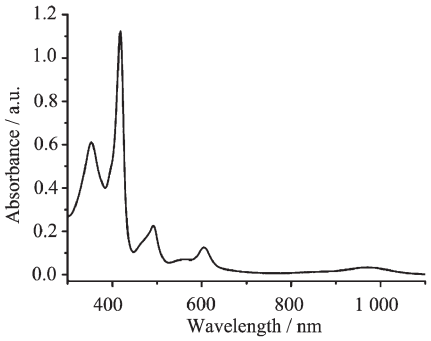

Fig.8　Electronic absorption spectrum of **2** in $CHCl_3$

bands observed at 2 924~2 927 cm^{-1} and 2 954~2 959 cm^{-1} in the IR spectrum of **1** due to the antisymmetric C-H stretching vibrations of the -CH_2- and -CH_3 groups, respectively[16].

2.3　Magnetic Properties

The dc magnetic properties of triple-deckers **1** and **2** are shown in Fig.10 under a 1 000 Oe field in the temperature range of 2 ~300 K. The effect of covalently incorporated POSS moieties at the porphyrin periphery on the magnetic behavior of the terbium triple-decker complexes is shown in Fig.10 by magnetic measurements over the sample of Tb_2(Pc)(TPP)$_2$ (**2**) diluted by Y_2(Pc)(TPP)$_2$ in the molar ratio of 1:9, isostructual to **2** according to XRD analysis (Fig. 11). The χ_mT value for per mol Tb_2 unit at 300 K is 23.68 $cm^3 \cdot K \cdot mol^{-1}$ for **1**, 23.88 $cm^3 \cdot K \cdot mol^{-1}$ for **2**, and 23.81 $cm^3 \cdot K \cdot mol^{-1}$ for the diluted sample of **2**, respectively, which are all consistent with the expected value of 23.62 $cm^3 \cdot K \cdot mol^{-1}$ for two Tb(Ⅲ) ions ($^7F_6$, S=3, L=3, g=3/2)[4b]. When the temperature is lowered, the χ_mT value of all the three samples decreases slowly until about 20 K, resulting from the

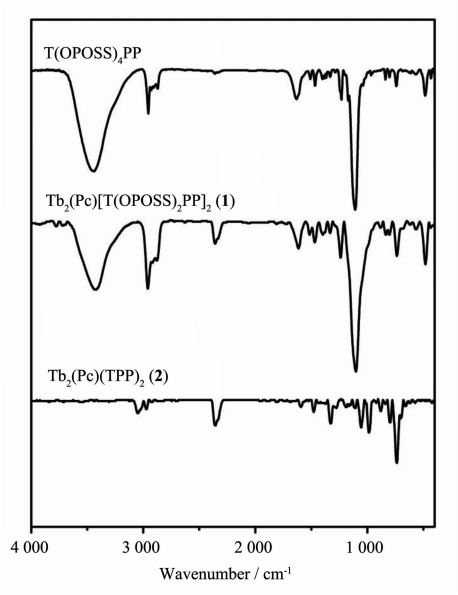

Fig.9　IR spectra of T(OPOSS)$_4$PP, **1** and **2**

crystal-field effects such as thermal depopulation of the lanthanide metal(Ⅲ) Stark sublevels. Then the χ_mT value increases quickly to reach a value of 22.04, 23.66, and 23.65 $cm^3 \cdot K \cdot mol^{-1}$ for **1**, **2**, and diluted sample of **2** at 2 K, respectively, indicating the presence of ferromagnetic interaction between two Tb (Ⅲ) ions in the triple-decker molecules [17]. However, at low temperature, the curve of **1** increases more quickly than that of **2**, probably owing to the weak antiferromagnetic interaction between the neighboring triple-deckers in **2** caused by the intermolecular dipole-dipole interaction. This is further verified by a qualitative manner according to the $\Delta\chi_mT$ tendency by subtracting the χ_mT of **1** from that of **2**, $\Delta\chi_mT_1$, as well as the $\Delta\chi_mT$ tendency by subtracting the χ_mT of diluted sample of **2** from that of **2**, $\Delta\chi_mT_2$. As shown in Fig.10, as the temperature lowers, the χ_mT value increases slowly until about 20 K, and then decreases quickly, confirming the presence of antiferromagnetic interaction between the neighboring triple-decker molecules of **2**. The change tendency of $\Delta\chi_mT_1$ is much faster than that of $\Delta\chi_mT_2$, indicating that connecting bulky inorganic POSS components at the porphyrin periphery of triple-decker compound leads to more obviously increase in the distance between neighboring triple-decker molecules and results in a more significant diminishment in the intermolecular interaction

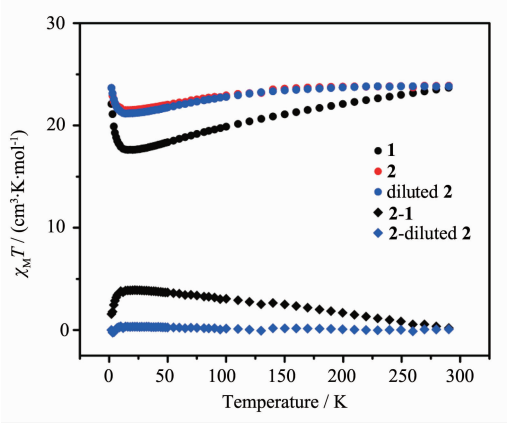

Fig.10 Temperature (T) dependence of $\chi_m T$ for compounds **1**, **2**, diluted **2**, **2**-**1**, and **2**-diluted **2** at 1000 Oe

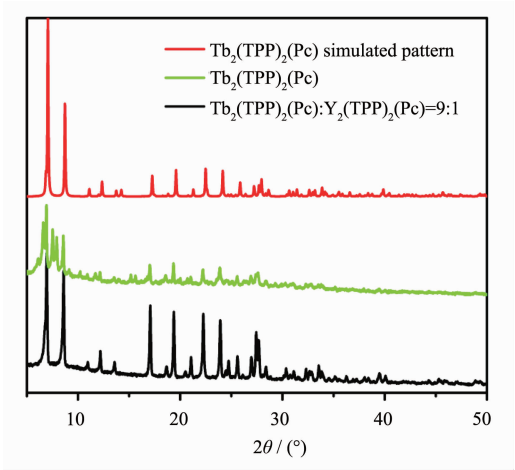

Fig.11 XRD patterns of **2** and diluted **2** together with simulated pattern from single crystal XRD data of **2**

between the triple-decker molecules than the physical dilution method. Fig.12 displays the magnetization (*M* vs *H*/*T*) curves for **1** and **2** at different temperatures (2, 3, 5 K), which shows a rapid increase tendency at low field and eventually reach the maximum value of 8.93μ_B for **1** and 6.09μ_B for **2** at 2 K, respectively, without achieving the magnetization saturation in terms of the expected saturation value of 18μ_B for two Tb(Ⅲ) ions (9μ_B for each Tb(Ⅲ) ion), indicating the presence of magnetic anisotropy and the crystal-field effect for the Tb(Ⅲ) ions.

Fig.13 shows temperature dependence of the in-phase (χ') and out-of-phase (χ'') ac susceptibility of $Tb_2(Pc)(TPP)_2$ (**2**) (A), diluted $Tb_2(Pc)(TPP)_2$ (**2**) with $Y_2(Pc)(TPP)_2$ at a molar ratio of 1∶9 (B), and $Tb_2(Pc)[T(OPOSS)_4PP]_2$ (**1**) (C), respectively, under zero Oe dc magnetic field in a 3.0 Oe ac field oscillating at 1.0~870 Hz. The in-phase signal (χ') of both $Tb_2(Pc)[T(OPOSS)_4PP]_2$ (**1**) and diluted sample of $Tb_2(Pc)(TPP)_2$ (**2**) with diamagnetic $Y_2(Pc)(TPP)_2$ shows the frequency-dependent character, revealing their SMM nature. This, however, is not true for $Tb_2(Pc)(TPP)_2$ (**2**). Obviously, introduction of the bulky POSS moieties onto the porphyrin periphery in the triple-decker compound **1** leads to the increase in the distance between neighboring triple-decker molecules, inducing a diminished intermolecular interactions between the triple-decker molecules and therefore showing the same effect over the magnetic behavior of triple-decker compound as done by diluting method. This result clearly indicates the advantage of connecting bulky inorganic POSS components at the porphyrin periphery of triple-decker compound in improving their magnetic properties.

As expected, with the help of the external direct current (dc) magnetic field, the frequency-dependent character in the in-phase signal (χ') and out-of-phase signal (χ'') becomes more obviously for both **1** and the diluted sample of **2**. Nevertheless, pure sample of triple-decker compound **2** without slow relaxation

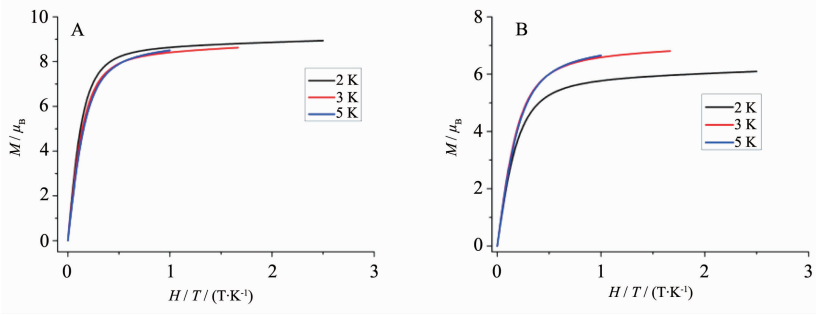

Fig.12 *M* vs. *H*/*T* curves for **1** (A) and **2** (B) at different temperatures

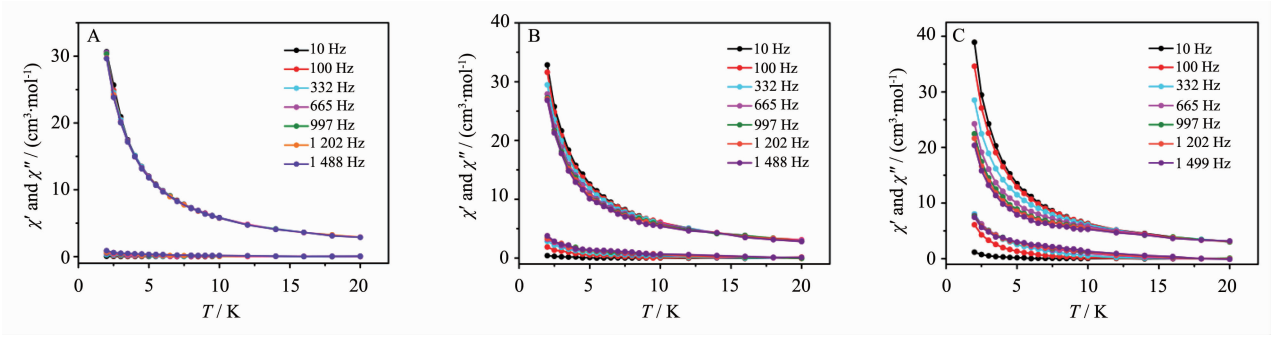

Fig.13　Temperature dependence of the in-phase (χ') and out-of-phase (χ'') ac susceptibility of $Tb_2(Pc)(TPP)_2$ (**2**) (A), diluted $Tb_2(Pc)(TPP)_2$ (**2**) with $Y_2(Pc)(TPP)_2$ at a molar ratio of 1:9 (B), and $Tb_2(Pc)[T(OPOSS)_4PP]_2$ (**1**) (C), respectively, under zero Oe dc magnetic field

behavior under zero Oe dc magnetic field does show the frequency-dependent character under the external dc magnetic field, indicating its field-induced SMM nature[3c,18]. On the basis of a thermally activated mechanism, $\tau=\tau_0 \exp[-U_{eff}/(kT)]$ and $\tau=1/(2\pi\upsilon)$, the Arrhenius law fitting for these picked peaks in χ vs. T curves for compounds **1**, **2**, and diluted sample of **2** under 3 000 Oe dc magnetic field is shown in Fig.14. A linear relationship exists between ln (τ) and $1/T$ for **1**, **2**, and diluted sample of **2**, which in turn results in the quite similar effective energy barrier of magnetization relaxation U_{eff}=14.4 cm^{-1} (20.7 K), 13.4

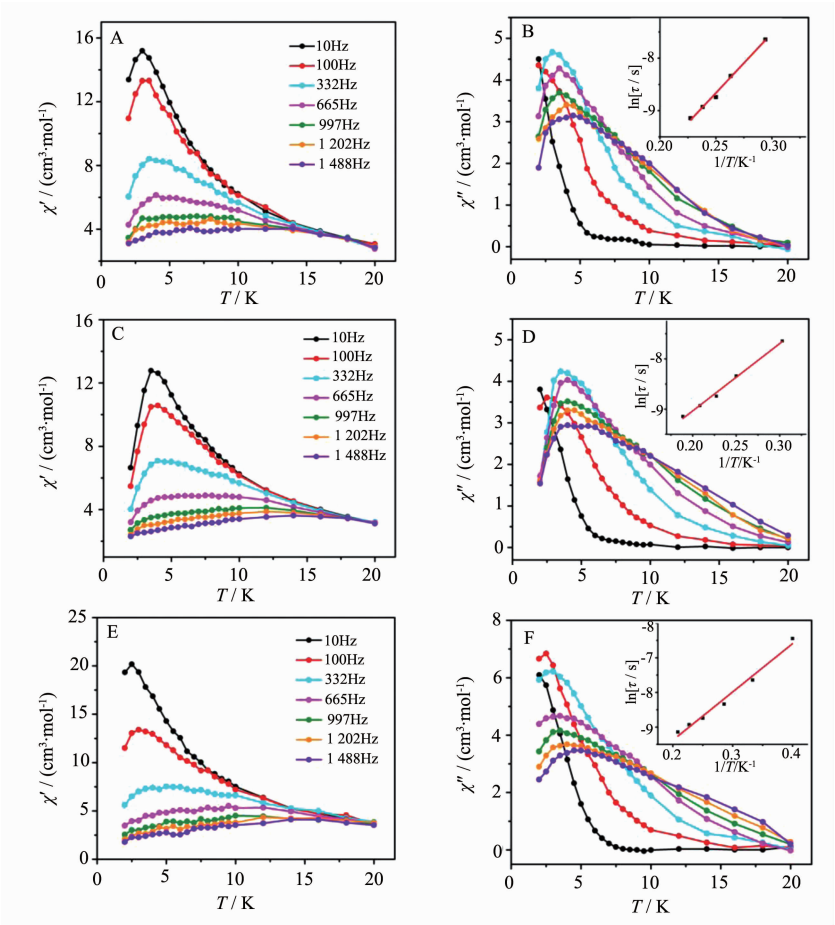

Fig.14　Temperature dependence of the in-phase (χ') and out-of-phase (χ'') ac susceptibility of $Tb_2(Pc)[T(OPOSS)_4PP]_2$ (**1**) (A, B), $Tb_2(Pc)(TPP)_2$ (**2**) (C, D) and diluted $Tb_2(Pc)(TPP)_2$ (**2**) with $Y_2(Pc)(TPP)_2$ at a molar ratio of 1:9 (E, F), respectively, under 3 000 Oe dc magnetic field

cm^{-1} (19.3 K), and 13.9 cm^{-1} (20.0 K) for **1**, **2**, and the diluted sample of **2** (but different relaxation time τ_0= 0.58, 8.2, and 5.3 μs) due to the effectively suppressing of the QTM with external direct current (dc) magnetic field in particular for the triple-decker compound **2**. This actually gives additional evidence for the effect of the covalently connecting bulky inorganic POSS components at the porphyrin periphery of triple-decker compound on separating the magnetic cores and diminishing the intermolecular interaction, which in turn improves the magnetic properties of the triple-decker SMM.

3 Conclusions

Intrinsic and field-induced SMM nature were revealed for the POSS-involved hybrid triple-decker sandwich-type complex Tb_2 (Pc) [T (OPOSS)$_4$PP]$_2$ and analogue Tb_2 (Pc) (TPP)$_2$, respectively, indicating the significant effect of covalently-linked, homogenously dispersed POSS moieties around the triple-decker core on improving the magnetic property of corresponding compounds.

Acknowledgements: Financial support from the Natural Science Foundation of China, National Key Basic Research Program of China (Grant No. 2013CB933402 and 2012CB224801), National Ministry of Education of China, and Beijing Municipal Commission of Education is gratefully acknowledged.

References:

[1] (a) Sessoli R, Tsai H, Schake A R, et al. *J. Am. Chem. Soc.*, **1993**,**115**:1804-1816
(b) Sessoli R, Gatteschi D, Caneschi A, et al. Nature, 1993,365:141-143;
(c) Woodruff D N, Winpenny R E P, Layfield R A. *Chem. Rev.*, **2013**,**113**:5110-5148

[2] (a) Leuenberger M N, Loss D. *Nature*, **2001**,**410**:789-793
(b) Ardavan A, Rival O, Morton J J L, et al. *Phys. Rev. Lett.*, **2007**,**98**:057201(1/2/3/4)
(c) Mannini M, Pineider F, Danieli C, et al. *Nature*, **2010**,**468**: 417-421
(d) Urdampilleta M, Nguyen N V, Cleuziou J P, et al. *Int. J. Mol. Sci.*, **2011**,**12**:6656-6667;
(e) Stamp P C E, Gaita-Arino A. *J. Mater. Chem.*, **2009**,**19**: 1718-1730

[3] (a) Habib F, Lin P, Long J, et al. *J. Am. Chem. Soc.*, **2011**, **133**:8830-8833
(b) Fukuda T, Matsumura K, Ishikawa N. *J. Phys. Chem. A*, **2013**,**117**:10447-10454
(c) Kan J, Wang H, Sun W, et al. *Inorg. Chem.*, **2013**,**52**: 8505-8510
(d) Wang H, Cao W, Liu T, et al. *Chem. Eur. J.*, **2013**,**19**: 2266-2270
(e) Zhang P, Guo Y, Tang J. *Coord. Chem. Rev.*, **2013**,**257**: 1728-1763;
(f) Wang H, Qian K, Wang K, et al. *Chem. Commun.*, **2011**, **47**:9624-9626

[4] (a) Titos-Padilla S, Ruiz J, Herrera J M, et al. *Inorg. Chem.*, **2013**,**52**:9620-9626
(b) Morita T, Katoh K, Breedlove B K, et al. *Inorg. Chem.*, **2013**,**52**:13555-13561
(c) Aronica C, Pilet G, Wernsdorfer W, et al. *Angew. Chem. Int. Ed.*, **2006**,**45**:4659-4662
(d) Guo Y, Xu G, Wernsdorfer W, et al. *J. Am. Chem. Soc.*, **2011**,**133**:11948-11951

[5] (a) Jiang S, Wang B, Su G, et al. *Angew. Chem. Int. Ed.*, **2010**,**49**:448-7451
(b) Ishikawa N, Sugita M, Wernsdorfer W. *J. Am. Chem. Soc.*, **2005**,**127**:3650-3651
(c) Wang H, Liu C, Liu T, et al. *Dalton. Trans.*, **2013**,**42**: 15355-15360

[6] (a) Meihaus K R, Long J R. *J. Am. Chem. Soc.*, **2013**,**135**: 17952-17957
(b) Lopez N, Prosvirin A. V, Zhao H, Wrnsdorfer W, et al. *Chem. Eur. J.*, **2009**,**15**:11390-11400
(c) Meihaus K R, Rinehart J D, Long J R. *Inorg. Chem.* **2011**,**50**:8484-8498
(d) Vergnani L, Barra A, Neugebauer P, et al. *Chem. Eur. J.*, **2012**,**18**:3390-3398

[7] Kumar A, Maji S, Dubey P, et al. *Tetrahedron Lett.*, **2007**,**48**:7287-7290

[8] Zhang W, Muller A H E. *Polymer*, **2010**,**51**:2133-2139

[9] Sun X, Li R, Wang D, et al. *Eur. J. Inorg. Chem.*, **2004**,**19**: 3806-3813

[10]Cordes D B, Lickiss P D, Rataboul F. *Chem. Rev.*, **2010**, **110**:2081-2173

[11](a) Jang K S, Kim H J, Johnson J R, et al. *Chem. Mater.*, **2011**,**23**:3025-3028
(b) Clarke D J, Matisons J G, Simon G P, et al. *Appl. Organomet. Chem.*, **2010**,**24**:184-188

(c) Xue Y, Liu Y, Lu F, et al. *J. Phys. Chem. Lett.*, **2012**,**3**: 1607-1612

[12]Sun J, Chen Y, Zhao L, et al. *Chem. Eur. J.*, **2013**,**19**: 12613-12618

[13]Katoh K, Horii Y, Yasuda N, et al. *Dalton Trans.*, **2012**,**41**: 13582-13600

[14]Sun X, Cui X, Arnold D P, et al. *Eur. J. Inorg. Chem.*, **2003**,**18**:1555-1561

[15](a) Jiang J, Arnold D P, Yu H. *Polyhedron*, **1999**,**18**:2129-2139

(b) Lu F, Bao M, Ma C, et al. *Spectrochim. Acta A*, **2003**, **59**:3273-3286

(c) Bao M, Pan N, Ma C, et al. *Vib. Spectrosc.*, **2003**,**32**: 175-184

[16]Shang H, Wang H, W. Wang K, et al, *Dalton Trans.*, **2013**,**42**:1109-1115

[17](a) Katoh K, Kajiwara T, Nakano M, et al. *Chem. Eur. J.*, **2011**,**17**:117-122

(b) Wang H, Liu T, Wang K, et al. *Chem. Eur. J.*, **2012**,**18**: 7691-7694

[18](a) Yamashita A, Watanabe A, Akine S, et al. *Angew. Chem. Int. Ed.*, **2011**,**50**:4016-4019

(b) Feltham H L C, Klower F, Cameron S. A, et al. *Dalton Trans.*, **2011**,**40**:11425-11432

(c) Koo B H, Lim K S, Ryu D W, et al. *Chem. Commun.*, **2012**,**48**:2519-2521

(d) Ruiz J, Lorusso G, Evangelisti M, et al. *Inorg. Chem.*, **2014**,**53**:3586-3594

(e) Chen L, Wang J, Wei J, et al. *J. Am. Chem. Soc.*, **2014**,**136**:12213-122